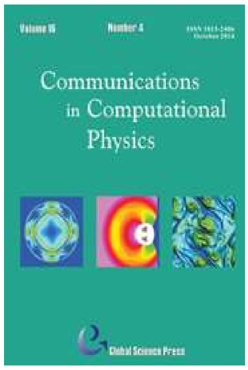

A New Coupled Complex Boundary Method for Bioluminescence Tomography

Rongfang Gong, Xiaoliang Cheng and Weimin Han

Communications in Computational Physics / Volume 19 / Issue 01 / January 2016, pp 226 - 250
DOI: 10.4208/cicp.230115.150615a, Published online: 15 January 2016

Commun. Comput. Phys.
doi: 10.4208/cicp.230115.150615a

Vol. **19**, No. 1, pp. 226-250
January 2016

A New Coupled Complex Boundary Method for Bioluminescence Tomography

Rongfang Gong[1,*], Xiaoliang Cheng[2] and Weimin Han[3,4]

[1] *Department of Mathematics, Nanjing University of Aeronautics and Astronautics, Nanjing 210016, China.*
[2] *Department of Mathematics, Zhejiang University, Hangzhou 310027, China.*
[3] *Department of Mathematics, University of Iowa, Iowa City, IA 52242, USA.*
[4] *School of Mathematics and Statistics, Xi'an Jiaotong University, Xi'an 710049, China.*

Received 23 January 2015; Accepted 15 June 2015

Abstract. In this paper, we introduce and study a new method for solving inverse source problems, through a working model that arises in bioluminescence tomography (BLT). In the BLT problem, one constructs quantitatively the bioluminescence source distribution inside a small animal from optical signals detected on the animal's body surface. The BLT problem possesses strong ill-posedness and often the Tikhonov regularization is used to obtain stable approximate solutions. In conventional Tikhonov regularization, it is crucial to choose a proper regularization parameter for trade off between the accuracy and stability of approximate solutions. The new method is based on a combination of the boundary condition and the boundary measurement in a parameter-dependent single complex Robin boundary condition, followed by the Tikhonov regularization. By properly adjusting the parameter in the Robin boundary condition, we achieve two important properties for our new method: first, the regularized solutions are uniformly stable with respect to the regularization parameter so that the regularization parameter can be chosen based solely on the consideration of the solution accuracy; second, the convergence order of the regularized solutions reaches one with respect to the noise level. Then, the finite element method is used to compute numerical solutions and a new finite element error estimate is derived for discrete solutions. These results improve related results found in the existing literature. Several numerical examples are provided to illustrate the theoretical results.

AMS subject classifications: 65N21, 65F22, 49J40, 74S05

Key words: Bioluminescence tomography, Tikhonov regularization, convergence rate, finite element methods, error estimate.

*Corresponding author. *Email addresses:* grf_math@nuaa.edu.cn (R. Gong), xiaoliangcheng@zju.edu.cn (X. Cheng), weimin-han@uiowa.edu (W. Han)

1 Introduction

Bioluminescence tomography (BLT) is a new molecular imaging modality and has shown its potential in monitoring non-invasively physiological and pathological processes *in vivo* at the cellular and molecular level. It is particularly attractive for *in vivo* applications because no external excitation source is needed and thus background noise is low while sensitivity is high [21]. In the BLT problem, one reconstructs quantitatively the bioluminescence source distribution inside a small animal from optical signals detected on the animal's body surface. Let $\Omega\subset\mathbb{R}^d$ ($d\leq 3$: space dimension) be an open bounded set with boundary $\Gamma:=\partial\Omega$. Then without going into detail, we state the BLT problem as follows.

Problem 1.1. Find a source function p inside Ω so that the solution u of the forward (real) Robin boundary value problem (BVP)

$$\begin{cases} -\mathrm{div}(D\nabla u)+\mu_a u=p & \text{in } \Omega, \\ u+2AD\frac{\partial u}{\partial n}=g^- & \text{on } \Gamma \end{cases} \tag{1.1}$$

satisfies the outgoing flux density on the boundary:

$$g=-D\frac{\partial u}{\partial n} \quad \text{on } \Gamma_0. \tag{1.2}$$

Here $D=[3(\mu_a+\mu')]^{-1}$ is the diffusion coefficient with μ_a and μ' being known as the absorption and reduced scattering parameters; $\partial/\partial n$ stands for the outward normal derivative; g^- is an incoming flux on Γ and it vanishes when the imaging is implemented in a dark environment; $\Gamma_0\subset\Gamma$ is the part of the boundary for measurement; $A=A(x)=(1+R(x))/((1-R(x)))$ with $R(x)\approx -1.4399\gamma(x)^{-2}+0.7099\gamma(x)^{-1}+0.6681+0.0636\gamma(x)$ and $\gamma(x)$ being the refractive index of the medium at $x\in\Gamma$. In what follows, we restrict ourselves to the case where $g^-\equiv 0$ and $\Gamma_0=\Gamma$.

Inverse source problems with only one measurement on the boundary do not have a unique solution. In the context of the BLT problem, one cannot distinguish between a strong source over a small region and a weak source over a large region. For instance, let Ω be the unit circle centered at the origin, $\mu_a=0.04$, $\mu'=1.5$, and $A=3.2$ with refractive index $\gamma=1.3924$. We assign two different source functions: a strong small source function $p_1=4$ in a circle centered $(0.5,0)$ with radius 0.2 and a weak big source function $p_2=1$ in a circle centered $(0.5,0)$ with radius 0.4. Although the solutions u_1 and u_2 of (1.1), corresponding to p_1 and p_2 respectively, differ greatly in Ω, they have almost the same outgoing flux density g on the boundary, as is shown in Fig. 1. This agrees with the theoretical result about the solution non-uniqueness presented in [12]. One can have better identification with more a priori information about the source function p. One of the a priori information is a permissible region $\Omega_0\subset\Omega$ of the optical source distribution. In this case, the first equation of (1.1) is replaced by

$$-\mathrm{div}(D\nabla u)+\mu_a u=p\chi_{\Omega_0} \quad \text{in } \Omega,$$

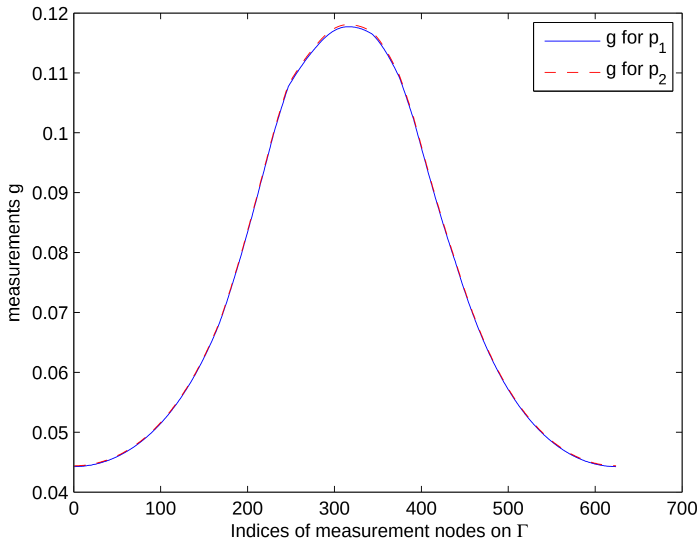

Figure 1: The outgoing flux on Γ for different source functions.

where χ_{Ω_0} is the characteristic function of Ω_0, i.e., its value is 1 in Ω_0, and is 0 outside Ω_0. Thus, the BLT problem is ill-posed. We refer the reader to [3, 6, 8, 9, 11–13, 16–20] etc. and references therein, for more theoretical analysis and numerical simulations on the BLT problem. We also refer to [14] for a detailed discussion of the theoretical aspects of general linear inverse source problems.

In this paper, we target for stable approximate solutions of Problem 1.1 using the Tikhonov regularization in a non-standard way. In the conventional Tikhonov regularization framework, the value of the regularization parameter is crucial to both solution accuracy and stability, and should be chosen carefully to balance these two aspects. One of the purposes of this work is to explore a new Tikhonov regularization method for solving Problem 1.1, with the property that the regularized solutions are insensitive with respect to the small size of the regularization parameter so that we can choose the regularization parameter based solely on the consideration of the solution accuracy. This will be accomplished by a parameter dependent coupled complex boundary method (CCBM) which reformulates Problem 1.1 into a complex one, see Section 2 for details. The parameter independent CCBM was first introduced in [4]. The idea of CCMB is to couple boundary conditions and boundary measurements into a Robin boundary condition in such a way that the Neumann data and Dirichlet data are the real part and imaginary part of the Robin boundary condition, respectively. As is shown in [4], the CCBM makes inverse source problems more robust and more efficient in computations. Different from [4], the parameter dependent CCBM proposed here includes a small parameter α in the coupled complex Robin boundary condition. As a result, when applying the Tikhonov regularization to the reformulated inverse problem, we can prove that with properly selected values of α, the regularized solutions are uniformly stable with respect to the regularization parameter.

Another contribution of this work is the possibility of improvement over the existing work about the convergence rate of linear inverse problems. Let K be the forward operator in our inverse problem and p^* be a solution for noise free data, to be defined in Section 3. It is well-known that under the source condition $p^* = K^*z$ for some z, the convergence rate is $\mathcal{O}(\sqrt{\delta})$; under the source condition $p^* = K^*Ky$ for some y, the convergence rate is $\mathcal{O}(\delta^{2/3})$, where K^* is the adjoint operator of K and δ is the noise level. Both convergence rates are optimal for these source conditions, see [15, Theorem 2.12] for example. For the new parameter dependent CCBM, we can prove a convergence rate $\mathcal{O}(\delta)$ when the source condition $p^* = K^*z$ for some z is satisfied and properly parameter α is chosen (cf. Theorem 3.3).

When piecewise constant functions are used to discretize the regularized problem, a finite element error estimate $\mathcal{O}(\varepsilon^{-1/2}h^{3/4}+\varepsilon^{-1/2}h^{1/2}E^h(p_\varepsilon^\delta)^{1/2})$ is shown in [12], where h is the finite element meshsize, ε is the regularization parameter and $E^h(p_\varepsilon^\delta)$ is defined in Theorem 4.2 of Section 4. In [4], with CCBM, the finite element error estimate is improved to $\mathcal{O}(\varepsilon^{-1}h^2+\varepsilon^{-1/2}h^{1/2}E^h(p_\varepsilon^\delta)^{1/2})$. However, in these error estimates, the magnitude of the error bounds can become very big when ε is small for an accurate reconstruction. In this paper, with parameter dependent CCBM and properly chosen parameter α, the error estimate is improved further to $\mathcal{O}(h^{2k+3/2}+h^{k+1/2}E^h(p_\varepsilon^\delta)^{1/2})$ with $k \geq 0$.

The paper is organized as follows. A detailed description of the parameter dependent CCBM is proposed in Section 2, where we also apply the Tikhonov regularization to the reformulated inverse problem to obtain stable approximate source functions. In Section 3, we provide a theoretical analysis of the new regularization framework. We discretize the regularized optimal problem with finite element methods in Section 4 and derive a new error estimate. Several numerical examples are presented in Section 5 to demonstrate the feasibility and efficiency of the proposed method. Finally, concluding remarks are given in Section 6.

2 A reformulation of the BLT problem with a new CCBM

We first introduce some notations for function spaces and assumptions on the data. For a set G (e.g., Ω, Ω_0 or Γ), we denote by $W^{m,s}(G)$ the standard real Sobolev spaces with the norm $\|\cdot\|_{m,s,G}$. Let $W^{0,s}(G) := L^s(G)$. In particular, $H^m(G)$ represents $W^{m,2}(G)$ with the corresponding inner product $(\cdot,\cdot)_{m,G}$ and norm $\|\cdot\|_{m,G}$. Let $\mathbf{H}^m(G)$ be the complex version of $H^m(G)$ with the inner product $((\cdot,\cdot))_{m,G}$ and norm $|||\cdot|||_{m,G}$ defined as follows: $\forall\, u,v \in \mathbf{H}^m(G)$, $((u,v))_{m,G} = (u,\bar{v})_{m,G}$, $|||v|||^2_{m,G} = ((v,v))_{m,G}$. Denote $V = H^1(\Omega)$, $\mathbf{V} = \mathbf{H}^1(\Omega)$, $Q = L^2(\Omega)$, $\mathbf{Q} = \mathbf{L}^2(\Omega)$, $Q_\Gamma = L^2(\Gamma)$, $\mathbf{Q}_\Gamma = \mathbf{L}^2(\Gamma)$ and $Q_0 = L^2(\Omega_0)$. The source function p will be sought from an admissible set $Q_{ad} \subset Q_0$. We assume Q_{ad} is nonempty, closed, and convex. For the problem data, assume Γ is Lipschitz continuous, $g \in Q_\Gamma$, and $D, \mu_a \in L^\infty(\Omega)$, $D \geq D_0$, $\mu_a \geq \mu_0$ a.e. in Ω for some positive constants D_0 and μ_0. In the following, we denote by c a constant which may have different values at different places.

Combining the boundary condition in (1.1) and measurement in (1.2), we have $u = 2Ag$ on Γ. Then Problem 1.1 reduces to finding a source function p in Ω_0 such that

$$\begin{cases} -\text{div}(D\nabla u)+\mu_a u = p\chi_{\Omega_0} & \text{in } \Omega, \\ D\frac{\partial u}{\partial n} = g_1, \quad u = g_2 & \text{on } \Gamma, \end{cases} \tag{2.1}$$

with $g_1 := -g$, $g_2 := 2Ag$.

For a parameter $\alpha > 0$, consider a complex BVP

$$\begin{cases} -\text{div}(D\nabla u)+\mu_a u = p\chi_{\Omega_0} & \text{in } \Omega, \\ D\frac{\partial u}{\partial n} + i\alpha u = g_1 + i\alpha g_2 & \text{on } \Gamma, \end{cases} \tag{2.2}$$

where $i = \sqrt{-1}$ is the imaginary unit. Obviously, if (u,p) satisfy (2.1), then (2.2) holds. Conversely, let (u,p) satisfy (2.2) and write $u = u_1 + iu_2$, u_1 and u_2 being the real and imaginary part of u. Then the real-valued functions u_1, u_2 satisfy

$$\begin{cases} -\text{div}(D\nabla u_1)+\mu_a u_1 = p\chi_{\Omega_0} & \text{in } \Omega, \\ D\frac{\partial u_1}{\partial n} - \alpha u_2 = g_1 & \text{on } \Gamma, \end{cases} \tag{2.3}$$

and

$$\begin{cases} -\text{div}(D\nabla u_2)+\mu_a u_2 = 0 & \text{in } \Omega, \\ D\frac{\partial u_2}{\partial n} + \alpha u_1 = \alpha g_2 & \text{on } \Gamma. \end{cases} \tag{2.4}$$

If $u_2 = 0$ in Ω, then $u_2 = 0, \frac{\partial u_2}{\partial n} = 0$ on Γ. As a result, from (2.3) and (2.4), it follows that $(u,p) = (u_1,p)$ satisfy (2.1) and hence also (1.1)-(1.2).

Summarizing the above discussion, we arrive at the following reformulation of the BLT problem.

Problem 2.1. Given g_1 and g_2, find $p \in Q_{ad}$ such that

$$u_2 = 0 \quad \text{in } \Omega,$$

where u_2 is the imaginary part of the solution $u = u_1 + iu_2$ of the BVP (2.2).

Define four bilinear forms:

$$a_\Omega(u,v) = \int_\Omega (D\nabla u \cdot \nabla v + \mu_a uv)dx \quad \forall u,v \in \mathbf{V}, \tag{2.5}$$

$$b_\Omega(u,v) = \int_\Omega uvdx \quad \forall u,v \in \mathbf{Q}, \tag{2.6}$$

$$b_{\Omega_0}(u,v) = \int_{\Omega_0} uvdx \quad \forall u,v \in \mathbf{Q}_0, \tag{2.7}$$

$$b_\Gamma(u,v) = \int_\Gamma uvds \quad \forall u,v \in \mathbf{Q}_\Gamma. \tag{2.8}$$

Note that the definitions in (2.5)-(2.8) are also valid when all the complex function spaces are replaced by the real ones. Then the weak form of (2.2) is

$$u\in\mathbf{V},\quad a_\Omega(u,\bar{v})+i\alpha b_\Gamma(u,\bar{v})=b_{\Omega_0}(p,\bar{v})+b_\Gamma(g_1+i\alpha g_2,\bar{v})\quad\forall v\in\mathbf{V}. \tag{2.9}$$

For a given $p\in Q_0$, by the use of the complex version of Lax-Milgram Lemma [7, p. 376], the problem (2.9) has a unique solution $u\in\mathbf{V}$. Moreover, we have

$$|||u|||_{1,\Omega}\le c(\|p\|_{0,\Omega_0}+\|g_1\|_{0,\Gamma}+\alpha\|g_2\|_{0,\Gamma}), \tag{2.10}$$

where $c>0$ is a constant independent of α. We refer to [4] for the proofs of the wellposedness of (2.9) and the priori estimate (2.10), with a slight modification due to the presence of the parameter α.

Next we apply the Tikhonov regularization to Problem 2.1 for stable approximation of a solution. In the following, we allow Neumann and Dirichlet data g_1 and g_2 to contain random noise with a known level δ, and write them as g_1^δ and g_2^δ. Then (2.2) is modified to

$$\begin{cases} -\mathrm{div}(D\nabla u^\delta)+\mu_a u^\delta=p\chi_{\Omega_0} & \text{in } \Omega,\\ D\frac{\partial u^\delta}{\partial n}+i\alpha u^\delta=g_1^\delta+i\alpha g_2^\delta & \text{on } \Gamma, \end{cases} \tag{2.11}$$

with

$$\|g_k^\delta-g_k\|_{0,\Gamma}\le\delta,\quad k=1,2.$$

The weak form of (2.11) is

$$u^\delta\in\mathbf{V},\quad a_\Omega(u^\delta,\bar{v})+i\alpha b_\Gamma(u^\delta,\bar{v})=b_{\Omega_0}(p,\bar{v})+b_\Gamma(g_1^\delta+i\alpha g_2^\delta,\bar{v})\quad\forall v\in\mathbf{V}. \tag{2.12}$$

For any $p\in Q_0$, denote by $u^\delta(p)=u_1^\delta(p)+iu_2^\delta(p)\in\mathbf{V}$ the solution of (2.12). Define a objective functional

$$J_\varepsilon^\delta(p)=\frac{1}{2}\|u_2^\delta(p)\|_{0,\Omega}^2+\frac{\varepsilon}{2}\|p\|_{0,\Omega_0}^2,$$

and introduce the following Tikhonov regularization framework for Problem 2.1.

Problem 2.2. Find $p_\varepsilon^\delta\in Q_{ad}$ such that

$$J_\varepsilon^\delta(p_\varepsilon^\delta)=\inf_{p\in Q_{ad}}J_\varepsilon^\delta(p).$$

It is not difficult to verify that for any $p,q\in Q_0$,

$$\begin{aligned}(J_\varepsilon^\delta)'(p)q&=(u_2^\delta(p),u_2^\delta(q)-u_2^\delta(0))_{0,\Omega}+\varepsilon(p,q)_{0,\Omega_0},\\ (J_\varepsilon^\delta)''(p)(q,q)&=\|u_2^\delta(q)-u_2^\delta(0)\|_{0,\Omega}^2+\varepsilon\|q\|_{0,\Omega_0}^2.\end{aligned}$$

Hence, for $\varepsilon>0$, $J_\varepsilon(\cdot)$ is strictly convex. Recall that Q_{ad} is non-empty, closed and convex. We have the following well-posedness result.

Proposition 2.1. For any $\varepsilon>0$, Problem 2.2 has a unique solution $p_\varepsilon^\delta\in Q_{ad}$ which depends continuously on all data. Moreover, p_ε is characterized by

$$(w_2^\delta+\varepsilon p_\varepsilon^\delta,q-p_\varepsilon^\delta)_{0,\Omega_0}\geq 0 \quad \forall q\in Q_{ad}, \tag{2.13}$$

where w_2^δ is the imaginary part of the weak solution $w^\delta:=w^\delta(p_\varepsilon^\delta)\in\mathbf{V}$ of the adjoint problem:

$$\begin{cases} -\mathrm{div}(D\nabla w^\delta)+\mu_a w^\delta=u_2^\delta & \text{in } \Omega, \\ D\frac{\partial w^\delta}{\partial n}+i\alpha w^\delta=0 & \text{on } \Gamma, \end{cases} \tag{2.14}$$

and u_2^δ is the imaginary part of the solution $u^\delta:=u^\delta(p_\varepsilon^\delta)\in\mathbf{V}$ of the BVP (2.12) with p replaced by p_ε^δ.

Proof of the well-posedness of Problem 2.2 is standard and we omit it here. The first order optimality condition (2.13) can be proved similar to [4, Proposition 3.1].

3 Convergence, uniform boundedness and improved convergence order

For the future need, we first prove the following lemma.

Lemma 3.1. *For any $p\in Q_0$, denote by $u(p)=u_1(p)+iu_2(p)$, $u^\delta(p)=u_1^\delta(p)+iu_2^\delta(p)\in\boldsymbol{V}$ the unique solutions of the problems* (2.9) *and* (2.12). *Then we have*

$$\|u_2^\delta(p)-u_2(p)\|_{1,\Omega}\leq c\alpha\delta. \tag{3.1}$$

Proof. Subtracting (2.9) from (2.12), we have,

$$a_\Omega(u^\delta(p)-u(p),\bar{v})+i\alpha b_\Gamma(u^\delta(p)-u(p),\bar{v})=b_\Gamma((g_1^\delta-g_1)+i\alpha(g_2^\delta-g_2),\bar{v}) \quad \forall v\in\mathbf{V}. \tag{3.2}$$

Similar to (2.10), applying the complex version of Lax-Milgram Lemma to (3.2), there holds

$$|||u^\delta(p)-u(p)|||_{1,\Omega}\leq c\left(\|g_1^\delta-g_1\|_{0,\Gamma}+\|g_2^\delta-g_2\|_{0,\Gamma}\right)\leq c\delta. \tag{3.3}$$

From (3.2), we have

$$a_\Omega(u_2^\delta(p)-u_2(p),v)=\alpha b_\Gamma((g_2^\delta-g_2)-(u_1^\delta(p)-u_1(p)),v) \quad \forall v\in V. \tag{3.4}$$

Take $v=u_2^\delta(p)-u_2(p)$ in (3.4) and use (3.3) to get (3.1). □

Denote by S the solution set of Problem 1.1 or 2.1, and assume it is nonempty. It is straightforward to show that S is closed and convex. Denote

$$p^*=\mathrm{arginf}_{p\in S}\|p\|_{0,\Omega_0}.$$

Then it exists and is unique. We have the following convergence result.

Theorem 3.1. *Fix $\alpha>0$. For a sequence of noise levels $\{\delta_n\}_{n\geq 1}$ which converges to 0 in $\mathbb{R}$ as $n\to\infty$, let $\varepsilon_n=\varepsilon(\delta_n)$ be chosen satisfying $\varepsilon_n\to 0$ and $\delta_n^2/\varepsilon_n\to 0$, as $n\to\infty$. Denote by $p_{\varepsilon_n}^{\delta_n}\in Q_{ad}$ the solution of Problem 2.2 with g_1^δ, g_2^δ and ε replaced by $g_1^{\delta_n}$, $g_2^{\delta_n}$ and ε_n respectively. Then the sequence $\{p_{\varepsilon_n}^{\delta_n}\}_{n\geq 1}$ converges to p^* in Q_0 as $n\to\infty$.*

Proof. For simplicity in exposition, write $p^n=p_{\varepsilon_n}^{\delta_n}$, $g_1^n=g_1^{\delta_n}$ and $g_2^n=g_2^{\delta_n}$. Denote by $u^n=u_1^n+iu_2^n=u^{\delta_n}(p^n)$ and $u^n(p^*)=u_1^n(p^*)+iu_2^n(p^*)$ the unique solutions of (2.12) in $\mathbf{V}$, both with g_1^δ, g_2^δ replaced by g_1^n, g_2^n, and with p replaced by p^n, p^* respectively. Moreover, from the definition of p^*, we have $u_2(p^*)=0$, $u_2(p^*)$ being the imaginary part of the solution of the problem (2.9) with p replaced by p^*. Then, using (3.1),

$$J_{\varepsilon_n}^{\delta_n}(p^n)\leq J_{\varepsilon_n}^{\delta_n}(p^*)=\frac{1}{2}\|u_2^n(p^*)-u_2(p^*)\|_{0,\Omega}^2+\frac{\varepsilon_n}{2}\|p^*\|_{0,\Omega_0}^2\leq c\alpha^2\delta_n^2+\frac{1}{2}\varepsilon_n\|p^*\|_{0,\Omega_0}^2,$$

which gives

$$\|p^n\|_{0,\Omega_0}^2\leq c\alpha^2\frac{\delta_n^2}{\varepsilon_n}+\|p^*\|_{0,\Omega_0}^2. \tag{3.5}$$

Like (2.10), we have the regularity estimate for u^n:

$$\begin{aligned}|||u^n|||_{1,\Omega}&\leq c(\|p^n\|_{0,\Omega_0}+\|g_1^n\|_{0,\Gamma}+\alpha\|g_2^n\|_{0,\Gamma})\\&\leq c(\|p^n\|_{0,\Omega_0}+\delta+\|g_1\|_{0,\Gamma}+\alpha\delta+\alpha\|g_2\|_{0,\Gamma}).\end{aligned} \tag{3.6}$$

From (3.5)-(3.6), $\{(p^n,u^n)\}$ is a bounded sequence in $Q_0\times\mathbf{V}$. Thus, there are a subsequence $\{n'\}$ of the sequence $\{n\}$ and some elements $p^\infty\in Q$, $u^\infty\in\mathbf{V}$ such that as $n'\to\infty$,

$$p^{n'}\rightharpoonup p^\infty \text{ in } Q_0,\quad u^{n'}\rightharpoonup u^\infty \text{ in } \mathbf{V},\quad u^{n'}\to u^\infty \text{ in } \mathbf{Q} \text{ and } \mathbf{Q}_\Gamma. \tag{3.7}$$

It is not difficult to verify that $u^\infty=u(p^\infty)$, the solution of (2.9) with p replaced by p^∞. In fact, from the definition of u^n, we have

$$a_\Omega(u^{n'},\bar{v})+i\alpha b_\Gamma(u^{n'},\bar{v})=a_{\Omega_0}(p^{n'},\bar{v})+b_\Gamma(g_1^{n'}+i\alpha g_2^{n'},\bar{v})\quad\forall v\in\mathbf{V}.$$

Let $n'\to 0$, and use the convergence relations (3.7) to get

$$a_\Omega(u^\infty,\bar{v})+i\alpha b_\Gamma(u^\infty,\bar{v})=a_{\Omega_0}(p^\infty,\bar{v})+b_\Gamma(g_1+i\alpha g_2,\bar{v})\quad\forall v\in\mathbf{V}.$$

This shows $u^\infty=u(p^\infty)$. Therefore, as $n'\to\infty$,

$$J_{\varepsilon_{n'}}^{\delta_{n'}}(p^{n'})=\frac{1}{2}\|u_2^{n'}\|_{0,\Omega}^2+\frac{\varepsilon_{n'}}{2}\|p^{n'}\|_{0,\Omega_0}^2\to\frac{1}{2}\|u_2(p^\infty)\|_{0,\Omega}^2,$$

where we used the boundedness of $\{p^{n'}\}_{n'}$ (cf. (3.5)). Since

$$J_{\varepsilon_{n'}}^{\delta_{n'}}(p^{n'})\leq J_{\varepsilon_{n'}}^{\delta_{n'}}(p^*)\leq c\alpha^2\delta_{n'}^2+\frac{1}{2}\varepsilon_{n'}\|p^*\|_{0,\Omega_0}^2\to 0\quad\text{as } n'\to\infty,$$

we arrive at the conclusion that

$$u_2(p^\infty)=0 \quad \text{in } \Omega.$$

As a result, p^∞ is a solution of Problem 2.1 or Problem 1.1. Hence, $p^\infty \in S$.

Next we prove $p^\infty = p^*$. From the lower semi-continuity of the norm $\|\cdot\|_{0,\Omega_0}$ and the weak convergence of $p^{n'}$ to p^∞, we have

$$\|p^\infty\|_{0,\Omega_0} \le \liminf_{n'\to\infty} \|p^{n'}\|_{0,\Omega_0}.$$

Therefore, for any fixed $\eta > 0$, there exists a positive integer N such that $\forall n' > N$, the following relation holds:

$$\|p^{n'}\|^2_{0,\Omega_0} \ge \|p^\infty\|^2_{0,\Omega_0} - \eta. \tag{3.8}$$

We note that (3.5) also holds when p^* is replaced by p^∞. Therefore, together with (3.8),

$$-\eta \le \|p^{n'}\|^2_{0,\Omega_0} - \|p^\infty\|^2_{0,\Omega_0} \le c\alpha^2 \frac{\delta^2_{n'}}{\varepsilon_{n'}}$$

holds for $n' > N$. Passing to the limit with $n' \to \infty$ first and then $\eta \to 0$ in the relation above to give

$$\lim_{n'\to\infty} \|p^{n'}\|_{0,\Omega_0} = \|p^\infty\|_{0,\Omega_0}. \tag{3.9}$$

From the definition of p^*, we have $\|p^*\|_{0,\Omega_0} \le \|p^\infty\|_{0,\Omega_0}$. Combining it with (3.5), for $n' > N$, the following relation holds:

$$\|p^{n'}\|^2_{0,\Omega_0} - \|p^\infty\|^2_{0,\Omega_0} \le \|p^{n'}\|^2_{0,\Omega_0} - \|p^*\|^2_{0,\Omega_0} \le c\alpha^2 \frac{\delta^2_{n'}}{\varepsilon_{n'}}.$$

Letting $n' \to \infty$ in the relation above and using (3.9), we have

$$\|p^\infty\|_{0,\Omega_0} = \|p^*\|_{0,\Omega_0}. \tag{3.10}$$

Using the definition of p^* again, (3.10) means $p^\infty = p^*$ and $p^{n'} \rightharpoonup p^*$ in Q, as $n' \to \infty$. Thus the limit does not depend on the subsequence selected, and then the entire solution sequence $p^n \rightharpoonup 0$ in Q, as $n' \to \infty$.

The strong convergence holds from $\lim_{n\to\infty} \|p^n\|_{0,\Omega_0} = \|p^*\|_{0,\Omega_0}$ and weak convergence, and the proof is completed. □

Denote by Π_{ad} the orthogonal projection from Q_0 onto Q_{ad}. Then the optimality condition (2.13) is equivalent to the following nonlinear equation:

$$p^\delta_\varepsilon = \Pi_{ad}\Big(-\frac{1}{\varepsilon} w^\delta_2 \chi_{\Omega_0}\Big). \tag{3.11}$$

We can ensure the uniform boundedness of $-\frac{1}{\varepsilon} w^\delta_2 \chi_{\Omega_0}$ by choosing the parameter α properly, as is shown next.

Theorem 3.2. *Let $\alpha=\mathcal{O}(\sqrt{\varepsilon})$. Then for any fixed $\delta\geq 0$, $-\frac{1}{\varepsilon}w_2^\delta\chi_{\Omega_0}$ is uniformly bounded in Q_0 with respect to ε for small $\varepsilon>0$.*

Proof. Denote by $u^\delta\in\mathbf{V}$ the solution of (2.12), with p replaced by p_ε^δ. Then using (3.5)-(3.6) and $\alpha=\mathcal{O}(\sqrt{\varepsilon})$, we have

$$\begin{aligned}|||u^\delta|||_{1,\Omega}&\leq c(\|p_\varepsilon^\delta\|_{0,\Omega_0}+\|g_1^\delta\|_{0,\Gamma}+\alpha\|g_2^\delta\|_{0,\Gamma})\\&\leq c\left(\delta\frac{\alpha}{\sqrt{\varepsilon}}+\|p^*\|_{0,\Omega_0}+\delta+\|g_1\|_{0,\Gamma}+\alpha\delta+\alpha\|g_1\|_{0,\Gamma}\right)\leq c.\end{aligned}\tag{3.12}$$

Let $u^\delta=u_1^\delta+iu_2^\delta$. Then $u_2^\delta\in V$ solve

$$a_\Omega(u_2^\delta,v)=\alpha b_\Gamma(g_2^\delta-u_1^\delta,v)\quad\forall v\in V.\tag{3.13}$$

Taking $v=u_2^\delta$ in (3.13) and using (3.12), we get

$$\|u_2^\delta\|_{1,\Omega}\leq c\alpha(\|u_1^\delta\|_{0,\Gamma}+\|g_2^\delta\|_{0,\Gamma})\leq c\alpha.\tag{3.14}$$

Similarly, from the definition of w^δ in (2.14), we have

$$|||w^\delta|||_{1,\Omega}\leq c\|u_2^\delta\|_{0,\Omega}\leq c\alpha.\tag{3.15}$$

Let $w^\delta=w_1^\delta+iw_2^\delta$. Then $w_2^\delta\in V$ solve

$$a_\Omega(w_2^\delta,v)=-\alpha b_\Gamma(w_1^\delta,v)\quad\forall v\in V.\tag{3.16}$$

Taking $v=u_2^\delta$ in (3.16) and using (3.15), we get

$$\|w_2^\delta\|_{1,\Omega}\leq c\alpha\|w_1^\delta\|_{0,\Gamma}\leq c\alpha^2.\tag{3.17}$$

Therefore, if $\alpha=\mathcal{O}(\sqrt{\varepsilon})$,

$$\left\|-\frac{1}{\varepsilon}w_2^\delta\chi_{\Omega_0}\right\|_{0,\Omega_0}=\mathcal{O}(1),$$

and the proof is completed. □

Theorem 3.2 indicates that a reasonable reconstruction of the source function can be achieved for rather small regularization parameter with a properly selected α. It also provides a guidance on how to choose α properly; see the numerical simulation results reported in Section 5.

Next we present a result on the convergence order of the regularized minimizer p_ε^δ to p^* as $\varepsilon\to 0$ and $\delta\to 0$.

For any $p\in Q_0$, denote $\tilde{u}(p)=\tilde{u}_1(p)+i\tilde{u}_2(p)=u^\delta(p)-u^\delta(0)\in\mathbf{V}$. Then $\tilde{u}(\cdot)$ is linear and we have

$$(\tilde{u}_2(p),z)_{0,\Omega}=(p,\tilde{w}_2)_{0,\Omega_0}\quad\forall p\in Q_0,\ z\in Q,\tag{3.18}$$

where $\tilde{w}_2\in V$ is the imaginary part of the weak solution $\tilde{w}=\tilde{w}_1+i\tilde{w}_2\in \mathbf{V}$ of the adjoint BVP

$$\begin{cases} -\mathrm{div}(D\nabla\tilde{w})+\mu_a\tilde{w}=z & \text{in } \Omega, \\ D\frac{\partial\tilde{w}}{\partial n}+i\alpha\tilde{w}=0 & \text{on } \Gamma. \end{cases} \tag{3.19}$$

We make the following assumption:

(A1) Assume there is $z^*\in Q$ such that $\tilde{w}_2^*\chi_{\Omega_0}=p^*$, where $\tilde{w}_2^*$ is the imaginary part of the weak solution $\tilde{w}^*=\tilde{w}_1^*+i\tilde{w}_2^*\in\mathbf{V}$ of the problem (3.19) with z replaced by z^*.

Note that Assumption (A1) is a source condition about p^*.

Theorem 3.3. *Let Assumption (A1) hold. Then, the solution p_ε^δ of Problem* 2.2 *satisfies the following estimate*

$$\|p_\varepsilon^\delta-p^*\|_{0,\Omega_0}\le c\Big(\sqrt{\varepsilon}+\frac{\alpha\delta}{\sqrt{\varepsilon}}\Big). \tag{3.20}$$

In particular, if $\varepsilon=\mathcal{O}(\delta^2)$ and $\alpha=\mathcal{O}(\sqrt{\varepsilon})$, then

$$\|p_\varepsilon^\delta-p^*\|_{0,\Omega_0}\le c\delta. \tag{3.21}$$

Proof. From the definitions of p_ε^δ and p^*, we have

$$J_\varepsilon^\delta(p_\varepsilon^\delta)=\frac{1}{2}\|u_2^\delta(p_\varepsilon^\delta)\|_{0,\Omega}^2+\frac{\varepsilon}{2}\|p_\varepsilon^\delta\|_{0,\Omega_0}^2\le J_\varepsilon^\delta(p^*)=\frac{1}{2}\|u_2^\delta(p^*)\|_{0,\Omega}^2+\frac{\varepsilon}{2}\|p^*\|_{0,\Omega_0}^2,$$

which gives

$$\|u_2^\delta(p_\varepsilon^\delta)\|_{0,\Omega}^2+\varepsilon\|p_\varepsilon^\delta-p^*\|_{0,\Omega_0}^2\le\|u_2^\delta(p^*)\|_{0,\Omega}^2-2\varepsilon(p^*,p_\varepsilon^\delta-p^*)_{0,\Omega_0}. \tag{3.22}$$

From (3.1), we obtain

$$\|u_2^\delta(p^*)\|_{0,\Omega}^2=\|u_2^\delta(p^*)-u_2(p^*)\|_{0,\Omega}^2\le c\alpha^2\delta^2, \tag{3.23}$$

where we used the fact that $u_2(p^*)=0$ in Ω.

In addition, from Assumption (A1) and by using (3.18), we have

$$(p^*,p_\varepsilon^\delta-p^*)_{0,\Omega_0}=(\tilde{w}_2^*,p_\varepsilon^\delta-p^*)_{0,\Omega_0}=(z^*,\tilde{u}_2(p_\varepsilon^\delta-p^*))_{0,\Omega}=(z^*,u_2^\delta(p_\varepsilon^\delta)-u_2^\delta(p^*))_{0,\Omega}. \tag{3.24}$$

Combine (3.22)-(3.24) to give

$$\|u_2^\delta(p_\varepsilon^\delta)\|_{0,\Omega}^2+2\varepsilon(z^*,u_2^\delta(p_\varepsilon^\delta))_{0,\Omega}+\varepsilon\|p_\varepsilon^\delta-p^*\|_{0,\Omega_0}^2\le c\alpha^2\delta^2+2\varepsilon(z^*,u_2^\delta(p^*))_{0,\Omega}. \tag{3.25}$$

By adding $\varepsilon^2\|z^*\|_{0,\Omega}^2$ to both sides of (3.25), we obtain

$$\|u_2^\delta(p_\varepsilon^\delta)+\varepsilon z^*\|_{0,\Omega}^2+\varepsilon\|p_\varepsilon^\delta-p^*\|_{0,\Omega_0}^2\le c\alpha^2\delta^2+2\varepsilon(z^*,u_2^\delta(p^*))_{0,\Omega}+\varepsilon^2\|z^*\|_{0,\Omega}^2. \tag{3.26}$$

Using (3.1) again,

$$(z^*,u_2^\delta(p^*))_{0,\Omega}=(z^*,u_2^\delta(p^*)-u_2(p^*))_{0,\Omega}\le c\alpha\delta\|z^*\|_{0,\Omega}.$$

Therefore, (3.26) implies

$$\|u_2^\delta(p_\varepsilon^\delta)+\varepsilon z^*\|_{0,\Omega}^2+\varepsilon\|p_\varepsilon^\delta-p^*\|_{0,\Omega_0}^2\le c\alpha^2\delta^2+2\varepsilon^2\|z^*\|_{0,\Omega}^2,$$

which leads to (3.20).

The bound (3.21) follows directly from (3.20) and the proof is completed. □

4 Finite element discretization and error estimates

In this section, we discretize Problem 2.2 and study the convergence of the numerical solutions. To simplify the notation, we omit in this section the symbol δ. We use linear finite elements to solve (2.12). For the source function p, piecewise constant approximations are used. For error estimation later, in this section, we assume $g_1,g_2\in H^{1/2}(\Gamma)$, and $\Omega\subset\mathbb{R}^d$ is a bounded open set with the boundary $\Gamma\in C^{1,1}$.

Let $\{\mathcal{T}_h\}_h$ be a regular family of finite element partitions of $\overline{\Omega}$. Define the linear finite element space

$$V^h=\{v\in C(\overline{\Omega})\,|\,v \text{ is linear in } T\ \forall T\in\mathcal{T}_h\}$$

and denote by $\pi^h v$ the piecewise linear interpolant of $v\in H^2(\Omega)$. Then we have the existence of a constant $c>0$ such that [1,2,5]

$$\|v-\pi^h v\|_{0,\Omega}+h\|v-\pi^h v\|_{1,\Omega}\le ch^2\|v\|_{2,\Omega}\quad\forall v\in H^2(\Omega).\tag{4.1}$$

Set $\mathbf{V}^h=V^h\oplus iV^h$. Then $\mathbf{V}^h$ is a finite element subspace of $\mathbf{V}$, and the finite element approximation of (2.12) is

$$a_\Omega(u^h,\bar{v}^h)+i\alpha b_\Gamma(u^h,\bar{v}^h)=b_{\Omega_0}(p,\bar{v}^h)+b_\Gamma(g_1+i\alpha g_2,\bar{v}^h)\quad\forall v^h\in\mathbf{V}^h.\tag{4.2}$$

Like the continuous case, the discrete problem (4.2) admit a unique solution $u^h\in\mathbf{V}^h$.

For any $p\in Q_0$, denote by $u\in\mathbf{V}$ and $u^h\in\mathbf{V}^h$ the solutions of (2.12) and (4.2). With arguments similar to those in [4, Section 4], we have $u\in\mathbf{H}^2(\Omega)$ and

$$|||u^h-u|||_{1,\Omega}\le ch|||u|||_{2,\Omega},\tag{4.3}$$

$$|||u^h-u|||_{0,\Omega}\le ch^2|||u|||_{2,\Omega}.\tag{4.4}$$

Here and below in this section, the constant c only depends on Ω, g_1, g_1 and p.

We will use the following inequality [2]:

$$\|v\|_{0,\Gamma}\le c\|v\|_{0,\Omega}^{1/2}\|v\|_{1,\Omega}^{1/2}\quad\forall v\in H^1(\Omega).\tag{4.5}$$

Lemma 4.1. *For any $p\in Q_0$, let $u=u_1+iu_2\in \boldsymbol{V}$ and $u^h=u_1^h+iu_2^h\in \boldsymbol{V}^h$ be the solutions of* (2.12) *and* (4.2) *respectively. Then the following error bounds hold:*

$$\|u_2^h-u_2\|_{1,\Omega}\le c\alpha h, \tag{4.6}$$
$$\|u_2^h-u_2\|_{0,\Omega}\le c\alpha h^{3/2}. \tag{4.7}$$

Proof. Recall that $u_2\in V$ and $u_2^h\in V^h$ satisfy

$$a_\Omega(u_2,v)+\alpha b_\Gamma(u_1,v)=\alpha b_\Gamma(g_2,v)\quad \forall v\in V, \tag{4.8}$$
$$a_\Omega(u_2^h,v^h)+\alpha b_\Gamma(u_1^h,v^h)=\alpha b_\Gamma(g_2,v^h)\quad \forall v^h\in V^h. \tag{4.9}$$

From (4.8) and (4.9),

$$a_\Omega(u_2^h-u_2,v^h)+\alpha b_\Gamma(u_1^h-u_1,v^h)=0\quad \forall v^h\in V^h.$$

Write

$$a_\Omega(u_2^h-u_2,u_2^h-u_2)=a_\Omega(u_2^h-u_2,v^h-u_2)+a_\Omega(u_2^h-u_2,u_2^h-v^h).$$

Then

$$a_\Omega(u_2^h-u_2,u_2^h-u_2)=a_\Omega(u_2^h-u_2,v^h-u_2)+I^h, \tag{4.10}$$

where

$$I^h=-\alpha b_\Gamma(u_1^h-u_1,u_2^h-v^h). \tag{4.11}$$

Note that from (2.4),

$$\|u_2\|_{2,\Omega}\le c\alpha \tag{4.12}$$

for some constant c independent of α.

We bound I^h of (4.11) as follows:

$$I^h\le\alpha\|u_1^h-u_1\|_{0,\Gamma}\left(\|u_2^h-u_2\|_{0,\Gamma}+\|v^h-u_2\|_{0,\Gamma}\right).$$

Apply (4.5) and (4.3), (4.4),

$$\|u_1^h-u_1\|_{0,\Gamma}\le c\|u_1^h-u_1\|_{0,\Omega}^{1/2}\|u_1^h-u_1\|_{1,\Omega}^{1/2}\le ch^{3/2}|||u|||_{2,\Omega}.$$

Thus,

$$I^h\le c\alpha h^{3/2}\|u_2^h-u_2\|_{1,\Omega}+c\alpha h^{3/2}\|v^h-u_2\|_{0,\Gamma}. \tag{4.13}$$

Now

$$||u_2^h-u_2||_{1,\Omega}^2\le ca_\Omega(u_2^h-u_2,u_2^h-u_2),$$

using (4.10) and (4.13), we have

$$\|u_2^h-u_2\|_{1,\Omega}^2\le c\|u_2^h-u_2\|_{1,\Omega}\|v^h-u_2\|_{1,\Omega}+c\alpha h^{3/2}\|u_2^h-u_2\|_{1,\Omega}+c\alpha h^{3/2}\|v^h-u_2\|_{0,\Gamma}.$$

By a standard argument,

$$\|u_2^h-u_2\|_{1,\Omega}\le c\inf_{v^h\in V^h}\Big[\|v^h-u_2\|_{1,\Omega}+c\alpha h^{3/2}+c(\alpha h^{3/2})^{1/2}\|v^h-u_2\|_{0,\Gamma}^{1/2}\Big].$$

Apply (4.5),

$$\|u_2^h-u_2\|_{1,\Omega}\le c\inf_{v^h\in V^h}\Big[\|v^h-u_2\|_{1,\Omega}+c\alpha h^{3/2}+c(\alpha h^{3/2})^{1/2}\|v^h-u_2\|_{1,\Omega}^{1/4}\|v^h-u_2\|_{0,\Omega}^{1/4}\Big].$$

Then

$$\begin{aligned}\|u_2^h-u_2\|_{1,\Omega}&\le c\Big(h\|u_2\|_{2,\Omega}+c\alpha h^{3/2}+c(\alpha h^{3/2})^{1/2}(h^{3/2}\|u_2\|_{2,\Omega})^{1/2}\Big)\\&\le c(\alpha h+\alpha h^{3/2})\end{aligned}$$

from which we obtain (4.6).

To prove (4.7), for any $r\in Q$, define $\varphi=\varphi(r)$ the solution of the BVP:

$$\begin{cases}-\mathrm{div}(D\nabla\varphi)+\mu_a\varphi=r & \text{in }\Omega,\\ D\frac{\partial\varphi}{\partial n}+\alpha\varphi=0 & \text{on }\Gamma.\end{cases}\tag{4.14}$$

For the solution regularity, we have

$$\|\varphi\|_{k,\Omega}\le c\|r\|_{0,\Omega},\quad k=1,2.\tag{4.15}$$

Combine (4.8), (4.9) and (4.14) to have

$$\begin{aligned}(u_2^h-u_2,r)_{0,\Omega}&=a_\Omega(u_2^h-u_2,\varphi)+\alpha b_\Gamma(u_2^h-u_2,\varphi)\\&=a_\Omega(u_2^h-u_2,\varphi-\pi^h\varphi)-\alpha b_\Gamma(u_1^h-u_1,\pi^h\varphi)+\alpha b_\Gamma(u_2^h-u_2,\varphi).\end{aligned}\tag{4.16}$$

Using (4.1), (4.6) and (4.15), we have

$$|a_\Omega(u_2^h-u_2,\varphi-\pi^h\varphi)|\le c\|u_2^h-u_2\|_{1,\Omega}\|\varphi-\pi^h\varphi\|_{1,\Omega}\le c\alpha h^2\|r\|_{0,\Omega}.\tag{4.17}$$

Applying the Cauchy-Schwarz inequality, (4.5), and (4.3)-(4.4), we have

$$|-\alpha b_\Gamma(u_1^h-u_1,\pi^h\varphi)|\le c\alpha\|u_1^h-u_1\|_{0,\Gamma}\|\pi^h\varphi\|_{0,\Gamma}\le c\alpha h^{3/2}\|r\|_{0,\Omega},\tag{4.18}$$

where we used $\|\pi^h\varphi\|_{0,\Gamma}\le\|\pi^h\varphi\|_{1,\Omega}\le\|\pi^h\varphi-\varphi\|_{1,\Omega}+\|\varphi\|_{1,\Omega}\le c\|r\|_{0,\Omega}$ for $h<1$.

Similarly, we have

$$|\alpha b_\Gamma(u_2^h-u_2,\varphi)|\le c\alpha^{3/2}h^{3/2}\|r\|_{0,\Omega}.\tag{4.19}$$

Then combining (4.16)-(4.19), we get

$$\|u_2^h-u_2\|_{0,\Omega}=\sup_{r\in Q}\frac{|(u_2^h-u_2,r)_{0,\Omega}|}{\|r\|_{0,\Omega}}\le c\alpha h^{3/2},$$

which gives (4.7), and the proof is completed. □

For any $p\in Q_0$, denote by $u^h(p)=u_1^h(p)+iu_2^h(p)\in\mathbf{V}^h$ the solution of (4.2). Define the discrete objective functional

$$J_\varepsilon^h(p)=\frac{1}{2}\|u_2^h(p)\|_{0,\Omega}^2+\frac{\varepsilon}{2}\|p\|_{0,\Omega_0}^2.$$

It is easy to verify that for $\varepsilon>0$, $J_\varepsilon^h(\cdot)$ is strictly convex.

For a full discretization of Problem 2.2, we approximate the source function p with piecewise constants. Define

$$Q_0^h=\{p\in Q_0\,|\,p \text{ is constant in } T,\ \forall T\in\mathcal{T}_h \text{ and } T\subset\overline{\Omega}_0\}$$

and the orthogonal projection operator $\Pi^h:Q_0\to Q_0^h$ by

$$(\Pi^h p,q^h)_{0,\Omega_0}=(p,q^h)_{0,\Omega_0}\quad\forall p\in Q,\ q^h\in Q_0^h. \tag{4.20}$$

Then there holds [5]:

$$\|p-\Pi^h p\|_{0,\Omega_0}\le ch|p|_{1,\Omega_0}\quad\forall p\in H^1(\Omega_0). \tag{4.21}$$

Set $Q_{ad}^h=Q_0^h\cap Q_{ad}$ and introduce the following discrete optimization problem:

Problem 4.1. Find $p_\varepsilon^h\in Q_{ad}^h$ such that

$$J_\varepsilon^h(p_\varepsilon^h)=\inf_{p^h\in Q_{ad}^h}J_\varepsilon^h(p^h).$$

Similar to Proposition 2.1, we have the following result on Problem 4.1.

Proposition 4.1. For any $\varepsilon>0$, Problem 4.1 has a unique solution $p_\varepsilon^h\in Q_{ad}^h$ which depends continuously on all data. Moreover, p_ε^h is characterized by the inequality

$$(w_2^h+\varepsilon p_\varepsilon^h,q^h-p_\varepsilon^h)_{0,\Omega_0}\ge 0\quad\forall q^h\in Q_{ad}^h, \tag{4.22}$$

where w_2^h is the imaginary part of weak solution $w^h:=w^h(p_\varepsilon^h)\in\mathbf{V}^h$ of the adjoint problem:

$$a_\Omega(w^h,\bar{v}^h)+i\alpha b_\Gamma(w^h,\bar{v}^h)=b_\Omega(u_2^h,\bar{v}^h)\quad\forall v^h\in\mathbf{V}^h. \tag{4.23}$$

and u_2^h is the imaginary part of the solution $u^h:=u^h(p_\varepsilon^h)\in\mathbf{V}^h$ of (4.2) with p replaced by p_ε^h.

Lemma 4.2. *For any $p\in Q_0$, let $w(p)$ be the solution of* (2.14) *and $w^h(p)$ be the solution of* (4.23), *with u_2^h being replaced by $u_2^h(p)$, which is the imaginary part of the solution of* (4.2). *Then*

$$|||w^h(p)-w(p)|||_{1,\Omega}\le c\alpha h, \tag{4.24}$$

$$|||w^h(p)-w(p)|||_{0,\Omega}\le c\alpha h^{3/2}. \tag{4.25}$$

Proof. Let $\tilde{w}^h := \tilde{w}^h(p) \in \mathbf{V}^h$ be the solution of

$$a_\Omega(\tilde{w}^h, \bar{v}^h) + i\alpha b_\Gamma(\tilde{w}^h, \bar{v}^h) = b_\Omega(u_2(p), \bar{v}^h) \quad \forall v^h \in \mathbf{V}^h, \tag{4.26}$$

where $u_2(p)$ is the imaginary part of the solution $u(p)$ of (2.12). Then using arguments similar to those in [4, Section 4] and noticing (3.14) and (3.15), we have

$$|||\tilde{w}^h(p) - w(p)|||_{1,\Omega} \le ch|||w(p)|||_{2,\Omega} \le c\alpha^2 h, \tag{4.27}$$

$$|||\tilde{w}^h(p) - w(p)|||_{0,\Omega} \le ch|||\tilde{w}^h(p) - w(p)|||_{1,\Omega} \le c\alpha^2 h^2. \tag{4.28}$$

Recall that $w^h := w^h(p)$ satisfies

$$a_\Omega(w^h, \bar{v}^h) + i\alpha b_\Gamma(w^h, \bar{v}^h) = b_\Omega(u_2^h(p), \bar{v}^h) \quad \forall v^h \in \mathbf{V}^h. \tag{4.29}$$

Subtract (4.26) from (4.29), take $v^h = w^h - \tilde{w}^h$ in the resulting equation and use (4.7) to give

$$|||w^h(p) - \tilde{w}^h(p)|||_{1,\Omega} \le c\|u_2^h - u_2\|_{0,\Omega} \le c\alpha h^{3/2}, \tag{4.30}$$

$$|||w^h(p) - \tilde{w}^h(p)|||_{0,\Omega} \le |||w^h(p) - \tilde{w}^h(p)|||_{1,\Omega} \le c\alpha h^{3/2}. \tag{4.31}$$

Then combining (4.27)-(4.28), (4.30)-(4.31) and using the triangle inequality,

$$|||w^h(p) - w(p)|||_{1,\Omega} \le |||w^h(p) - \tilde{w}^h(p)|||_{1,\Omega} + |||\tilde{w}^h(p) - w(p)|||_{1,\Omega},$$

$$|||w^h(p) - w(p)|||_{0,\Omega} \le |||w^h(p) - \tilde{w}^h(p)|||_{0,\Omega} + |||\tilde{w}^h(p) - w(p)|||_{0,\Omega},$$

we obtain (4.24) and (4.25). The proof is completed. □

We can prove sharper estimates about the imaginary part of $w^h(p) - w(p)$, given in the following lemma.

Lemma 4.3. *For any $p \in Q_0$, let $w(p)$ and $w^h(p)$ be defined in Lemma 4.2. In addition, let $w(p) = w_1(p) + iw_2(p)$ and $w^h(p) = w_1^h(p) + iw_2^h(p)$. Then we have*

$$\|w_2^h(p) - w_2(p)\|_{1,\Omega} \le c\alpha^2 h, \tag{4.32}$$

$$\|w_2^h(p) - w_2(p)\|_{0,\Omega} \le c\alpha^2 h^{3/2}. \tag{4.33}$$

Proof. Recall that $\tilde{w}^h(p) = \tilde{w}_1^h(p) + i\tilde{w}_2^h(p)$ solves (4.26). Then $\tilde{w}_2^h := \tilde{w}_2^h(p)$ satisfies

$$a_\Omega(\tilde{w}_2^h, v^h) + \alpha b_\Gamma(\tilde{w}_1^h, v^h) = 0 \quad \forall v^h \in V^h. \tag{4.34}$$

Similarly, $w_2^h := w_2^h(p) \in V^h$ satisfies

$$a_\Omega(w_2^h, v^h) + \alpha b_\Gamma(w_1^h, v^h) = 0 \quad \forall v^h \in V^h. \tag{4.35}$$

Subtract (4.34) from (4.35), take $v^h = w_2^h - \tilde{w}_2^h$ in the resulting equation, and using (4.31) as well as (4.5) to get

$$||w_2^h(p) - \tilde{w}_2^h(p)||_{1,\Omega} \le c\alpha\|w_1^h(p) - \tilde{w}_1^h(p)\|_{0,\Gamma} \le c\alpha^2 h^{3/2}. \tag{4.36}$$

Combining (4.27)-(4.28) and (4.36), and applying the triangle inequality, we obtain (4.32) and (4.33). □

Next we give an error estimate for the light source function p_ε with respect to h as follows.

Theorem 4.2. *For fixed $\varepsilon>0$ and $\delta\ge 0$, let $p_\varepsilon^\delta\in Q_{ad}$ be the solution of Problem* 2.2 *and $p_\varepsilon^h\in Q_{ad}^h$ be the solution of Problem* 4.1. *Then*

$$\|p_\varepsilon^h-p_\varepsilon^\delta\|_{0,\Omega_0}\le c\,(\alpha^2\varepsilon^{-1}h^{3/2}+\alpha\varepsilon^{-1/2}h^{1/2}E^h(p_\varepsilon)^{1/2}), \tag{4.37}$$

where $E^h(p_\varepsilon^\delta)=\|\Pi^h p_\varepsilon^\delta-p_\varepsilon^\delta\|_{0,\Omega_0}=\inf_{q^h\in Q_{ad}^h}\|q^h-p_\varepsilon^\delta\|_{0,\Omega_0}$.

Proof. Let $\hat{p}_\varepsilon^h\in Q_{ad}^h$ be the unique solution of Problem 4.1 with $J_\varepsilon^h(\cdot)$ replaced by $J_\varepsilon(\cdot)$. Then

$$(w_2(\hat{p}_\varepsilon^h)+\varepsilon\hat{p}_\varepsilon^h,q^h-\hat{p}_\varepsilon^h)_{0,\Omega_0}\ge 0\quad\forall q^h\in Q_{ad}^h, \tag{4.38}$$

where $w_2(\hat{p}_\varepsilon^h)$ is the imaginary part of the weak solution of the BVP (2.14) with u_2^δ being replaced by $u_2(\hat{p}_\varepsilon^h)$, which is the imaginary part of the solution $u(\hat{p}_\varepsilon^h)$ of (2.12). We can verify $\hat{p}_\varepsilon^h\to p_\varepsilon^\delta$ as $h\to 0$.

Replace q in (2.13) with $\hat{p}_\varepsilon^h$ and q^h in (4.38) with $\Pi^h p_\varepsilon^\delta$, and add the resulting inequalities to get

$$\varepsilon\|\hat{p}_\varepsilon^h-p_\varepsilon^\delta\|_{0,\Omega_0}^2\le(w_2(\hat{p}_\varepsilon^h)+\varepsilon\hat{p}_\varepsilon^h,\Pi^h p_\varepsilon^\delta-p_\varepsilon^\delta)_{0,\Omega_0}+(w_2(\hat{p}_\varepsilon^h)-w_2(p_\varepsilon^\delta),p_\varepsilon^\delta-\hat{p}_\varepsilon^h)_{0,\Omega_0}. \tag{4.39}$$

Using (4.20), (4.21), and noticing $w_2(\hat{p}_\varepsilon^h)\chi_{\Omega_0}\in H^1(\Omega_0)$, we have

$$\begin{aligned}(w_2(\hat{p}_\varepsilon^h)+\varepsilon\hat{p}_\varepsilon^h,\Pi^h p_\varepsilon^\delta-p_\varepsilon^\delta)_{0,\Omega_0}&=(w_2(\hat{p}_\varepsilon^h)-\Pi^h w_2(\hat{p}_\varepsilon^h)\chi_{\Omega_0},\Pi^h p_\varepsilon^\delta-p_\varepsilon^\delta)_{0,\Omega_0}\\&\le c\|w_2(\hat{p}_\varepsilon^h)\|_{1,\Omega}E^h(p_\varepsilon^\delta)\le c\alpha^2 hE^h(p_\varepsilon^\delta),\end{aligned} \tag{4.40}$$

where we apply (3.17) and use the uniform boundedness of $\hat{p}_\varepsilon^h$ with respect to h since $\hat{p}_\varepsilon^h\to p_\varepsilon^\delta$ as $h\to 0$.

Moreover, with arguments similar to those in [4, Theorem 4.4], we can prove

$$(w_2(\hat{p}_\varepsilon^h)-w_2(p_\varepsilon^\delta),p_\varepsilon^\delta-\hat{p}_\varepsilon^h)_{0,\Omega_0}=-\|u_2(\hat{p}_\varepsilon^h)-u_2(p_\varepsilon^\delta)\|_{0,\Omega}^2. \tag{4.41}$$

Combine (4.39)-(4.41) to obtain

$$\|u_2(\hat{p}_\varepsilon^h)-u_2(p_\varepsilon^\delta)\|_{0,\Omega}^2+\varepsilon\|\hat{p}_\varepsilon^h-p_\varepsilon^\delta\|_{0,\Omega_0}^2\le c\alpha^2 hE^h(p_\varepsilon^\delta). \tag{4.42}$$

Similarly, replace q^h in (4.22) with $\hat{p}_\varepsilon^h$ and q^h in (4.38) with p_ε^h, and add the resulting inequalities to get

$$\begin{aligned}\varepsilon\|p_\varepsilon^h-\hat{p}_\varepsilon^h\|_{0,\Omega_0}^2&\le(w_2(\hat{p}_\varepsilon^h)-w_2^h(p_\varepsilon^h),p_\varepsilon^h-\hat{p}_\varepsilon^h)_{0,\Omega_0}\\&\le(w_2(\hat{p}_\varepsilon^h)-w_2(p_\varepsilon^h),p_\varepsilon^h-\hat{p}_\varepsilon^h)_{0,\Omega_0}+(w_2(p_\varepsilon^h)-w_2^h(p_\varepsilon^h),p_\varepsilon^h-\hat{p}_\varepsilon^h)_{0,\Omega_0}.\end{aligned} \tag{4.43}$$

Applying (4.33), we have

$$\begin{aligned}|(w_2(p_\varepsilon^h)-w_2^h(p_\varepsilon^h),p_\varepsilon^h-\hat{p}_\varepsilon^h)_{0,\Omega_0}|&\le c\|w_2(p_\varepsilon^h)-w_2^h(p_\varepsilon^h)\|_{0,\Omega}\|p_\varepsilon^h-\hat{p}_\varepsilon^h\|_{0,\Omega_0}\\&\le c\alpha^2 h^{3/2}\|p_\varepsilon^h-\hat{p}_\varepsilon^h\|_{0,\Omega_0}.\end{aligned} \tag{4.44}$$

Using arguments similar to those in the proof of [4, Theorem 4.4], there holds

$$(w_2(\hat{p}_\varepsilon^h)-w_2(p_\varepsilon^h),p_\varepsilon^h-\hat{p}_\varepsilon^h)_{0,\Omega_0}=-\|u_2(p_\varepsilon^h)-u_2(\hat{p}_\varepsilon^h)\|_{0,\Omega}^2. \tag{4.45}$$

Then combine (4.43)-(4.45) to give

$$\|u_2(p_\varepsilon^h)-u_2(\hat{p}_\varepsilon^h)\|_{0,\Omega}^2+\varepsilon\|p_\varepsilon^h-\hat{p}_\varepsilon^h\|_{0,\Omega_0}^2\le c\alpha^2h^{3/2}\|p_\varepsilon^h-\hat{p}_\varepsilon^h\|_{0,\Omega_0}. \tag{4.46}$$

Consequently, from (4.42) and (4.46) as well as triangle inequality

$$\|p_\varepsilon^h-p_\varepsilon^\delta\|_{0,\Omega_0}\le\|p_\varepsilon^h-\hat{p}_\varepsilon^h\|_{0,\Omega_0}+\|\hat{p}_\varepsilon^h-p_\varepsilon^\delta\|_{0,\Omega_0},$$

we obtain the error bound (4.37). □

Corollary 4.1. *For fixed $\varepsilon>0$ and $\delta\ge0$, let $p_\varepsilon^\delta\in Q_{ad}$ be the solution of Problem* 2.2 *and $p_\varepsilon^h\in Q_{ad}^h$ be the solution of Problem* 4.1. *Furthermore, assume $p_\varepsilon^\delta\in H^1(\Omega_0)$ and set $\alpha=\mathcal{O}(\sqrt{\varepsilon}h^k)$ with $k\ge0$. Then*

$$\|p_\varepsilon^h-p_\varepsilon^\delta\|_{0,\Omega_0}\le c(h^{2k+3/2}+h^{k+1}\|p_\varepsilon^\delta\|_{1,\Omega_0}). \tag{4.47}$$

Proof. Applying (4.21) and substituting $\alpha=\mathcal{O}(\sqrt{\varepsilon}h^k)$ in (4.37) to give (4.47). □

5 Numerical results

We present in this section some numerical results based on our parameter dependent CCBM. The goal is to illustrate the theoretical results presented in the previous sections, i.e., the uniform stability of the regularized solutions in Q_0 with respect to the regularization parameter ε, the first order convergence of the regularized solutions with respect to the noise level δ, and the finite element error estimate of the regularized solutions with respect to the meshsize h.

Given Ω, let $\mathcal{T}_h,h,V^h,Q_0^h$ and Π^h be defined as in Section 4. For a triangulation $\mathcal{T}_h$, let E and N denote the numbers of its elements and nodes. We assume the source function p is sought in the natural set $Q_{ad}:=\{q\in Q_0\,|\,q\ge0 \text{ a.e. in } \Omega_0\}$. In this situation, the projection Π_{ad} of (3.11) reduces to

$$p_\varepsilon^\delta=\max\Big\{-\frac{1}{\varepsilon}w_2^\delta\chi_{\Omega_0},0\Big\}.$$

To focus on the test of our theoretical results, assume we know exactly the location of the true source function which means $\Omega_0=\Omega_*$, the support of the true light source function, so that the fast method suggested in [10] can be applied. Specifically, we solve first the system of equations:

$$\begin{cases} a_\Omega(\nabla u_1^h,v^h)-\alpha b_\Gamma(u_2^h,v^h)+\frac{1}{\varepsilon}b_{\Omega_0}(w_2^h,v^h)=b_\Gamma(g_1^\delta,v^h) & \forall v^h\in V^h,\\ \alpha b_\Gamma(u_1^h,v^h)+a_\Omega(u_2^h,v^h)=\alpha b_\Gamma(g_2^\delta,v^h) & \forall v^h\in V^h,\\ -b_\Omega(u_2^h,v^h)+a_\Omega(w_1^h,v^h)-\alpha b_\Gamma(w_2^h,v^h)=0 & \forall v^h\in V^h,\\ \alpha b_\Gamma(w_1^h,v^h)+a_\Omega(w_2^h,v^h)=0 & \forall v^h\in V^h, \end{cases} \tag{5.1}$$

and then compute

$$p_\varepsilon^h = \Pi^h \left(-\frac{1}{\varepsilon} w_2^h \chi_{\Omega_0} \right). \tag{5.2}$$

5.1 Example 1

Data preparation In the first example, let the problem domain $\Omega = \{(x,y) \in \mathbb{R}^2 \mid x^2+y^2 < 1\}$. The absorption and reduced scattering coefficients in Ω are $\mu_a = 0.0088$ and $\mu' = 1.001$ respectively. Then the diffusion coefficient $D = [3(\mu_a+\mu')]^{-1} \approx 0.3301$. Let the refractive index on Γ be $\gamma = 1.3924$. So $A = 3.2$. Place a light source with an intensity $p^* = 1$ in the region $\Omega_* = \{(x,y) \in \Omega \mid (x-0.4)^2+(y-0.25)^2 \leq 0.2^2\}$. Solve the forward BVP (1.1) with finite element method:

$$a_\Omega(u^h, v^h) + \frac{1}{2A} b_\Gamma(u^h, v^h) = b_{\Omega_*}(p^*, v^h), \quad \forall v^h \in V^h, \tag{5.3}$$

on a fine mesh with $h = 0.0124$, $E = 296960$, $N = 139025$, and compute measurement $g = -D\frac{\partial u^h}{\partial n}$ on Γ. For a noise level δ, a uniformly distributed random noise is added to g to get g^δ. Set $g_1^\delta = -g^\delta$ and $g_2^\delta = 2Ag^\delta$.

Reconstruction For given Ω, $\Omega_0 = \Omega_*$, D, μ_a, A, g_1^δ and g_2^δ, (5.1) and (5.2) are implemented to recover p_ε^h for different regularization parameter ε, noise level δ and grid parameter h. Recalling Theorems 3.2, 3.3 and 4.2, in this example, we set the parameter $\alpha = \sqrt{\varepsilon}$.

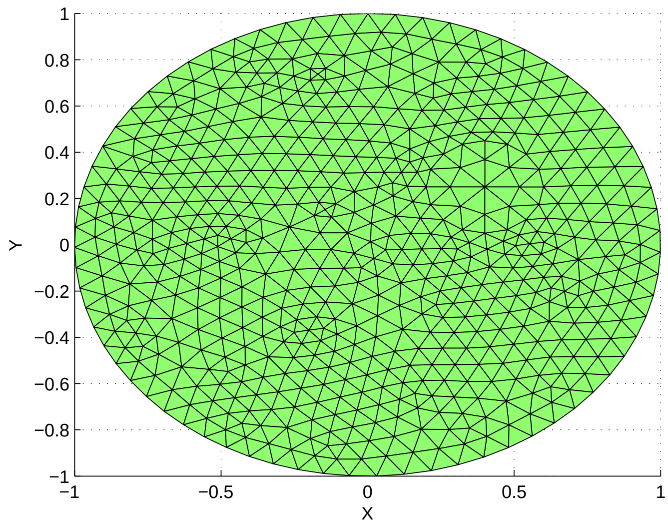

Figure 2: A sketch of mesh.

Table 1: The uniformity of the approximate solutions with respect to ε.

ε	$\delta=4^{-1}$	$\delta=4^{-2}$	$\delta=4^{-3}$	$\delta=4^{-4}$	$\delta=4^{-5}$
10^{-1}	5.9321e-1	5.1651e-1	4.9734e-1	4.9254e-1	4.9134e-1
10^{-2}	2.0796e-1	5.8470e-2	2.1110e-2	1.1783e-2	9.4567e-3
10^{-3}	1.9997e-1	4.8964e-2	1.1225e-2	1.8771e-3	8.6123e-4
10^{-4}	1.9989e-1	4.8864e-2	1.1222e-2	1.7779e-3	9.3312e-4
10^{-5}	1.9988e-1	4.8863e-2	1.1220e-2	1.7766e-3	9.3409e-4
10^{-6}	1.9988e-1	4.8863e-2	1.1220e-2	1.7765e-3	9.3412e-4
10^{-7}	1.9988e-1	4.8863e-2	1.1220e-2	1.7763e-3	9.3411e-4
10^{-8}	1.9988e-1	4.8863e-2	1.1220e-2	1.7765e-3	9.3409e-4
10^{-9}	1.9988e-1	4.8863e-2	1.1220e-2	1.7765e-3	9.3413e-4
10^{-10}	1.9988e-1	4.8863e-2	1.1220e-2	1.7766e-3	9.3410e-4
10^{-11}	1.9985e-1	4.8863e-2	1.1220e-2	1.7766e-3	9.3411e-4
10^{-12}	1.9988e-1	4.8875e-2	1.1220e-2	1.7763e-3	9.3203e-4
10^{-13}	1.9988e-1	4.8863e-2	1.1220e-2	1.7765e-3	9.3427e-4
10^{-14}	1.9989e-1	4.8863e-2	1.1220e-2	1.7766e-3	9.3403e-4
10^{-15}	1.9989e-1	4.8863e-2	1.1220e-2	1.7765e-3	9.3439e-4
10^{-16}	1.9988e-1	4.8897e-2	1.1220e-2	1.7767e-3	9.3476e-4
10^{-17}	1.9988e-1	4.8896e-2	1.1221e-2	1.7764e-3	8.7232e-4
10^{-18}	1.9988e-1	4.8863e-2	1.1220e-2	1.7743e-3	9.3976e-4
10^{-19}	1.9988e-1	4.8863e-2	1.1221e-2	1.7786e-3	9.3404e-4
10^{-20}	1.9989e-1	4.8863e-2	1.1118e-2	1.7770e-3	9.4008e-4

We first examine the uniform stability of the approximate source functions with respect to ε when δ and h are fixed. Specifically, for fixed but different $\delta=4^{-1}, 4^{-2}, 4^{-3}, 4^{-4}$ and 4^{-5}, p_ε^h are computed for different ε on a mesh with meshsize $h=0.03837$, $E=18560$ and $N=9417$, and the relative errors of p_ε^h in L^2-norm, defined as

$$\text{L2Err} := \frac{\|p_\varepsilon^h - p^*\|_{0,\Omega_0}}{\|p^*\|_{0,\Omega_0}}, \tag{5.4}$$

are listed in Table 1. We conclude from Table 1 that for a fixed meshsize and a noise level, the approximate source functions obtained from our new parameter dependent CCBM are uniformly stable with respect to the regularization parameter.

We then test the error estimates in Theorem 4.2 and Corollary 4.1. Recall that the error estimates in Theorem 4.2 and Corollary 4.1 are about $\|p_\varepsilon^h - p_\varepsilon^\delta\|_{0,\Omega_0}$. However, in practice, we cannot compute it because we do not know p_ε^δ. Due to

$$\|p_\varepsilon^h - p_\varepsilon^\delta\|_{0,\Omega_0} \le \|p_\varepsilon^h - p^*\|_{0,\Omega_0} + \|p^* - p_\varepsilon^\delta\|_{0,\Omega_0},$$

we can use L2Err in (5.4) to estimate $\|p_\varepsilon^h - p_\varepsilon^\delta\|_{0,\Omega_0}$ when $\|p^* - p_\varepsilon^\delta\|_{0,\Omega_0}$ is small enough. According to the convergence of p_ε^δ to p^* as $\delta,\varepsilon \to 0$, $\|p^* - p_\varepsilon^\delta\|_{0,\Omega_0}$ can be very small as long

Table 2: Convergence order in h.

h (E,N)	0.2187 (190,163)	0.1185 (1160,615)	0.06743 (4640,2389)	0.03837 (18560,9417)
L2Err	1.0243e-1	2.4537e-2	5.4780e-3	9.4008e-4
Conv. order	-	2.3320	2.6594	3.1261

as both δ and ε are small enough. In conventional methods, the regularization parameter can not be very small because of the ill-posedness of the problems. However, with our method, ε can be very small due to the uniform stability of the solutions with respect to ε. Specifically, in this example, we set $\delta=2^{-10}$ and $\varepsilon=10^{-20}$, for instance. We reconstruct the source functions for $h=0.2187$, 0.1185, 0.06743 and 0.03837. The corresponding L2Err and convergence order with respect to h are reported in Table 2. We can see from Tables 2 that in this example, the numerical convergence orders of the discrete solutions with respect to h are better than those claimed in Corollary 4.1.

Finally, we test the convergence order of solutions with respect to the noise level δ under the assumption of the source condition (A1). Specifically, given $z^*(x,y)=-|x+y|$ in Ω, we solve,

$$\begin{cases} a_\Omega(w_1^h,v^h)-\alpha b_\Gamma(w_2^h,\bar{v}^h)=b_\Omega(z^*,v^h) & \forall v^h\in V^h, \\ \alpha b_\Gamma(w_1^h,\bar{v}^h)+a_\Omega(w_2^h,v^h)=0 & \forall v^h\in V^h, \end{cases} \tag{5.5}$$

and then set

$$p^*(\alpha)=w_2^h\chi_{\Omega_0}. \tag{5.6}$$

Here we use $p^*(\alpha)$ rather than p^* to show the dependence of true source function on the parameter α. For a given δ, the Neumann and Dirichlet data g_1^δ and g_2^δ are obtained again through solving (5.3), with p^* replaced by $p^*(\alpha)$. As suggested by Theorem 3.3, set $\varepsilon=\delta^2$. Let $\delta=4^{-k}$, $k=1,2,\cdots,5$, and the approximate source functions denoted by $p_\varepsilon^h(\alpha)$ are constructed from (5.1)-(5.2), on the mesh with $h=0.03837$, $E=18560$ and $N=9417$. The corresponding relative errors and convergence orders are listed in Table 3. It is shown in Table 3 that the convergence order of $p_\varepsilon^h(\alpha)$ with respect to δ approaches to 1 when δ is getting smaller. This confirms the result stated in Theorem 3.3.

Table 3: Convergence order in δ.

δ	4^{-1}	4^{-2}	4^{-3}	4^{-4}	4^{-5}
L2Err	1.1383e-1	5.5533e-2	1.4290e-2	3.5741e-3	8.9353e-4
Conv. order	–	0.5177	0.9792	0.9997	1.0000

5.2 Example 2

Data preparation In the second example, we consider a 3D problem with a boundary Γ that is not $C^{1,1}$ smooth. Specifically, let $\Omega = \{(x,y,z) \in \mathbb{R}^3 \mid x^2+y^2<1, 0<z<2\}$. In Ω, let $\mu_a = 0.0052$, $\mu' = 1.081$ and thus $D = 0.3069$. The refractive index on the boundary Γ is γ=1.3314 and thus A=2.8. Place a light source with an intensity $p^*(x,y,z) = 1+(x-0.5)^2+(y-0.5)^2+(z-1)^2$ in the region $\Omega_* = \{(x,y,z) \in \Omega \mid (x-0.5)^2+(y-0.5)^2+(z-1)^2 \leq 0.2^2\}$. Then (5.3) is solved again on a mesh with $h = 0.1130$, $E = 314982$ and $N = 55269$ to obtain light flux density g on the boundary. Uniformly distributed random noise with δ is also added to g to get g^δ. Let $g_1^\delta = -g^\delta$ and $g_2^\delta = 2Ag^\delta$.

Reconstruction Again, for given Ω, $\Omega_0 = \Omega_*$, D, μ_a, A, g_1^δ and g_2^δ above, equations (5.1) and (5.2) are solved to obtain approximate source functions p_ε^h for different ε, δ and h. Like in the first example, set $\alpha = \sqrt{\varepsilon}$.

For given δ, p_ε^h is recovered on a mesh with meshsize $h = 0.2285$, $E = 26885$, $N = 5023$, and the errors L2Err of p_ε^h are reported in Table 4. Again, we can see from Table 4 that for constant h and δ, the approximate source functions are uniformly stable with respect to the regularization parameters ε.

To examine the error estimates of p_ε^h with respect to meshsize h, fix $\delta = 2^{-10}$ and $\varepsilon = 10^{-20}$. We reconstruct source functions on the meshes with $h = 0.5293$, 0.4162, 0.2828 and 0.2285, respectively. The corresponding L2Err and convergence orders with respect to h are computed and shown in Table 5. Tables 5 indicates that the convergence order is bigger than 1 when the mesh is not fine, and it decreases as h is getting smaller. The

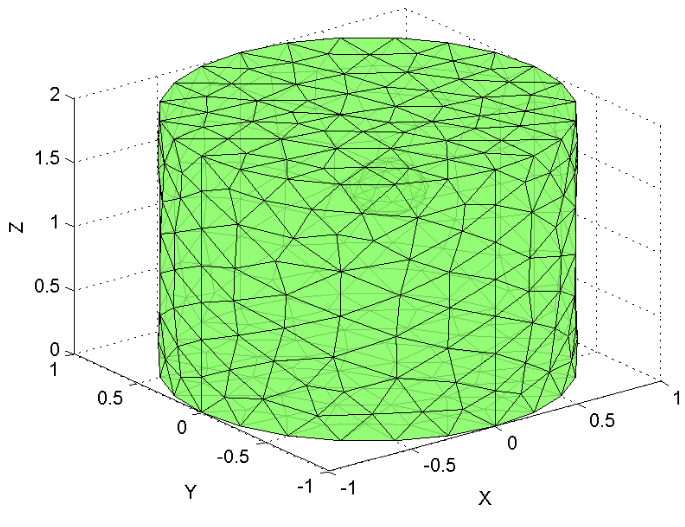

Figure 3: A sketch of mesh.

Table 4: Relative L^2-norm error in reconstructed source function.

ε	$\delta=4^{-1}$	$\delta=4^{-2}$	$\delta=4^{-3}$	$\delta=4^{-4}$	$\delta=4^{-5}$
10^{-1}	8.8401e-1	8.9116e-1	8.9295e-1	8.9340e-1	8.9351e-1
10^{-2}	5.0832e-2	1.0935e-1	1.2740e-1	1.3198e-1	1.3313e-1
10^{-3}	1.5898e-1	7.5833e-2	5.9676e-2	5.6410e-2	5.5658e-2
10^{-4}	1.6098e-1	7.7325e-2	6.0802e-2	5.7403e-2	5.6615e-2
10^{-5}	1.6100e-1	7.7338e-2	6.0810e-2	5.7410e-2	5.6621e-2
10^{-6}	1.6100e-1	7.7338e-2	6.0810e-2	5.7410e-2	5.6621e-2
10^{-7}	1.6100e-1	7.7338e-2	6.0810e-2	5.7410e-2	5.6621e-2
10^{-8}	1.6100e-1	7.7338e-2	6.0810e-2	5.7410e-2	5.6621e-2
10^{-9}	1.6100e-1	7.7338e-2	6.0810e-2	5.7410e-2	5.6621e-2
10^{-10}	1.6100e-1	7.7338e-2	6.0810e-2	5.7410e-2	5.6621e-2
10^{-11}	1.6100e-1	7.7338e-2	6.0810e-2	5.7410e-2	5.6621e-2
10^{-12}	1.6100e-1	7.7338e-2	6.0810e-2	5.7410e-2	5.6621e-2
10^{-13}	1.6100e-1	7.7338e-2	6.0810e-2	5.7410e-2	5.6621e-2
10^{-14}	1.6100e-1	7.7338e-2	6.0810e-2	5.7410e-2	5.6621e-2
10^{-15}	1.6100e-1	7.7338e-2	6.0810e-2	5.7410e-2	5.6621e-2
10^{-16}	1.6100e-1	7.7338e-2	6.0810e-2	5.7410e-2	5.6621e-2
10^{-17}	1.6100e-1	7.7338e-2	6.0810e-2	5.7410e-2	5.6621e-2
10^{-18}	1.6100e-1	7.7338e-2	6.0810e-2	5.7410e-2	5.6621e-2
10^{-19}	1.6100e-1	7.7338e-2	6.0810e-2	5.7410e-2	5.6621e-2
10^{-20}	1.6100e-1	7.7338e-2	6.0810e-2	3.1570e-2	5.6621e-2

Table 5: Convergence order in h.

h (E,N)	0.5293 (2212,488)	0.4162 (4836,998)	0.2828 (13895,2666)	0.2285 (26885,5023)
L2Err	1.6891e-1	1.0913e-1	6.8126e-2	5.6621e-2
Conv. order	-	1.8172	1.2193	0.8676

reason is that when h is small enough, the finite element error is not the main component in the total error which also contains other errors such as error in data and error from regularization etc.

For $\delta=4^{-k}$, $k=1,2,\cdots,5$, set $\varepsilon=\delta^2$. Assume the source condition (A1) holds. Given $z^*=-1$ in Ω, solve (5.5)-(5.6) to give $p^*(\alpha)$. Again, the Neumann and Dirichlet data g_1^δ, g_2^δ are obtained by solving (5.3), with p^* replaced by $p^*(\alpha)$. The experiments are repeated on the mesh with $h=0.2285$, and the results are shown in Table 6. Again, Table 6 indicates the convergence order of $p_\varepsilon^h(\alpha)$ with respect to δ in this example confirms the result stated in Theorem 3.3 as δ is getting smaller.

Table 6: Convergence order w.r.t. δ.

δ	4^{-1}	4^{-2}	4^{-3}	4^{-4}	4^{-5}
L2Err	8.1246e-1	2.2345e-2	1.2801e-2	3.2289e-3	8.0735e-4
Conv. order	–	2.5921	0.4018	0.9936	0.9999

6 Conclusions

In this paper, we propose a parameter dependent CCBM-based Tikhonov regularization method for an inverse source problem arising from bioluminescence tomography. As shown by theory and numerical examples, one major strength of our method is that the approximate source functions are uniformly stable with respect to the regularization parameter. This is advantageous because otherwise one will have to pay careful attention on the choice of the regularization parameter for trade off between the solution accuracy and stability. Moreover, with the help of the small parameter α, we improve the existing work on the convergence order of the regularized solutions with respect to the noise level and the error estimates of finite element solutions with respect to the meshsize. We note that the method explored here can be applied directly to general real elliptic inverse source problems with boundary conditions and measurements which can be transformed into Dirichlet and Neumann data.

Acknowledgments

We thank the two anonymous referees for their careful review of our manuscript and for their constructive comments. The work of the first author was supported by the Natural Science Foundation of China (Grant No. 11401304), the Natural Science Foundation of Jiangsu Province (Grant No. BK20130780), and the Fundamental Research Funds for the Central Universities (Grant No. NS2014078). The work of the second author was supported by the Key Project of the Major Research Plan of NSFC (Grant No. 91130004). The work of the third author was partially supported by NSF (Grant No. DMS-1521684) and Simons Foundation (Grant No. 207052 and 228187).

References

[1] K. Atkinson and W. Han, Theoretical Numerical Analysis: A Functional Analysis Framework, Third edition, Springer-Verlag, New York, 2009.
[2] S. C. Brenner and L. R. Scott, The Mathematical Theory of Finite Element Methods, Third edition, Springer-Verlag, New York, 2008.
[3] X. L. Cheng, R. F. Gong and W. Han, A new general mathematical framework for bioluminescence tomography, Comput. Methods Appl. Mech. Engrg., 197 (2008), 524-535.
[4] X. L. Cheng, R. F. Gong, W. Han and X. Zheng, A novel coupled complex boundary method for solving inverse source problems, Inverse Probl., 30 (2014), 055002 20pp.

[5] P. G. Ciarlet, The Finite Element Method for Elliptic Problems, North-Holland, Amsterdam, 1978.

[6] W. X. Cong, G. Wang, D. Kumar *et al.*, Practical reconstrucion method for bioluminescence tomography, Opt. Express, 18 (2005), 6756-6771.

[7] R. Dautray and J. L. Lions, Mathematical Analysis and Numerical Methods for Science and Technology, Vol. 2, Springer, Berlin, 1988.

[8] J. Feng, C. Qin, S. Zhu *et al.*, Total variation regularization for bioluminescence tomography with the split Bregman method, Appl. Opt., 51 (2012), 4501-4512.

[9] R. F. Gong, X. L. Cheng and W. Han, Theorectical analysis and numerical realization of bioluminesecne tomography, J. Concrete Appl. Math., 8 (2010), 504-527.

[10] R. F. Gong, X. L. Cheng and W. Han, A fast solver for an inverse problem arising in bioluminesecne tomography, J. Comp. Appl. Math., 267 (2014) 228-243.

[11] W. Guo, K. Jia, D. Han *et al.*, Efficient sparse reconstruction algorithm for bioluminescence tomography based on duality and variable splitting, Appl. Opt., 51 (2002), 5676-5685.

[12] W. Han, W. X. Cong and G. Wang, Mathematical theory and numerical analysis of bioluminescence tomography, Inverse Probl., 22 (2006), 1659-1675.

[13] X. W. He, Y. B. Hou, D. F. Chen *et al.*, Sparse regularization-based reconstruction for bioluminescence tomography using a multilevel adaptive finite element method, Int. J. Biomed. Imag. 2011 (2011), 203537 11 pages.

[14] V. Isakov, Inverse Source Problems, American Mathematical Society, New York, 1990.

[15] A. Kirsch, An Introduction to the Mathematical Theory of Inverse Problems, Springer, New York, 1996.

[16] T. Kreutzmann, Geometric Regularization in Bioluminescence Tomography, KIT Scientific Publishing, 2014.

[17] K. Liu, J. Tian, Y. Lu *et al.*, A fast bioluminescent source localization method based on generalized graph cuts with mouse model validations, Opt. Express, 18 (2010), 3732-3745.

[18] Y. Lv, J. Tian, W. Cong *et al.*, A multilevel adaptive finite element algorithm for bioluminescence tomography, Opt. Express, 14 (2006), 8211-8223

[19] G. Wang, Y. Li and M. Jiang, Uniqueness theorems in bioluminescence tomography, Med. Phys., 31 (2004), 2289-2299.

[20] T. Wang, S. Gao, L. Zhang *et al.*, Overlap domain decomposition method for bioluminescence tomography (BLT), Commun. Numer. Meth. Engng., 26 (2010), 511-523.

[21] R. Weissleder and V. Ntziachristos, Shedding light onto live molecular targets, Nat. Med., 9 (2003), 123-128.